ResearchGate

See discussions, stats, and author profiles for this publication at: https://www.researchgate.net/publication/231241135

Cu(II) Oxide Amorphous Nanoclusters Grafted Ti3+ Self-Doped TiO2: An Efficient Visible Light Photocatalyst

ARTICLE *in* CHEMISTRY OF MATERIALS · NOVEMBER 2011

Impact Factor: 8.35 · DOI: 10.1021/cm203025b

CITATIONS
89

READS
129

4 AUTHORS:

Min Liu
The University of Tokyo
31 PUBLICATIONS **760** CITATIONS
SEE PROFILE

Xiaoqing Qiu
Fuzhou University
46 PUBLICATIONS **1,126** CITATIONS
SEE PROFILE

Masahiro Miyauchi
Tokyo Institute of Technology
96 PUBLICATIONS **3,477** CITATIONS
SEE PROFILE

Kazuhito Hashimoto
The University of Tokyo
528 PUBLICATIONS **29,183** CITATIONS
SEE PROFILE

Available from: Min Liu
Retrieved on: 17 January 2016

CHEMISTRY OF MATERIALS

Article

pubs.acs.org/cm

Cu(II) Oxide Amorphous Nanoclusters Grafted Ti^{3+} Self-Doped TiO_2: An Efficient Visible Light Photocatalyst

Min Liu,[‡] Xiaoqing Qiu,[‡] Masahiro Miyauchi,*[,†] and Kazuhito Hashimoto*[,‡,§]

[†]Department of Metallurgy and Ceramics Science, Graduate School of Science and Engineering, Tokyo Institute of Technology, 2-12-1 Ookayama, Meguro-ku, Tokyo 152-8552, Japan

[‡]Research Center for Advanced Science and Technology, The University of Tokyo, 4-6-1 Komaba, Meguro-ku, Tokyo 153-8904, Japan

[§]Graduate School of Engineering, The University of Tokyo, 7-3-1 Hongo, Bunkyo-ku, Tokyo 113-8656, Japan

Supporting Information

ABSTRACT: Ti^{3+} self-doped TiO_2 was prepared by a facile one-step thermal oxidation of Ti_2O_3 and TiO_2 mixture in air. Electron spin resonance (ESR) spectra confirmed the presence of Ti^{3+} in this sample. Ti^{3+} states caused a visible light absorption, which is originated from the isolated band in its forbidden gap. Although the photocatalytic activity of this Ti^{3+} self-doped TiO_2 was negligible even under the UV light, its UV and visible light activities were drastically increased by the grafting of Cu(II) oxide amorphous clusters with a size of around 2 nm as a co-catalyst. Consequently, the photocatalytic decomposition of gaseous 2-propanol (IPA) into CO_2 with a maximum generation rate of 0.20 μmol/h and a quantum efficiency of 10.8% is achieved, under the visible light irradiation. Its efficient visible light activity is highly stable in air and can be repeatedly used for a long term.

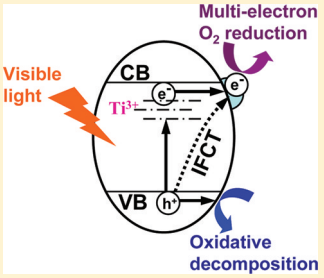

KEYWORDS: *Ti^{3+}, Cu(II) oxide amorphous nanoclusters, IFCT, visible light sensitive, photocatalysis*

INTRODUCTION

Titanium dioxide (TiO_2) has attracted much attention during the past years, owing to its wide applications in photocatalysis.[1,2] However, TiO_2 can only be activated under UV light irradiation because of its large band gap, 3.2 eV for anatase and 3.0 eV for rutile.[2] Therefore, a great deal of effort has been made to modify the band structure of TiO_2 to make it sensitive to visible light. The introduction of Ti^{3+} states has been reported as an effective way to extend the light absorption of TiO_2-based materials into visible light.[3] However, a Ti^{3+} defect has been widely considered as a recombination center for the photogenerated electrons and the lowering the photocatalytic activity,[4] owing to the fact that its energy level is located in the intraband,[5] as well as the low electron mobility in these sites.[6]

Our group designed a visible-light-sensitive photocatalyst by grafting Cu(II) or Fe(III) amorphous clusters onto TiO_2 surfaces.[7] X-ray absorption fine structure (XAFS) analysis revealed that Cu(II) oxide or Fe(III) hydroxide amorphous nanoclusters formed on the TiO_2 surface.[7] Visible light irradiation initiates interfacial charge transfer (IFCT) from the valence band (VB) of TiO_2 to the surface nanoclusters. In the case of Cu(II) oxide amorphous nanoclusters modified TiO_2 (Cu(II)-TiO_2), electrons in the valence band of TiO_2 can be directly excited to Cu(II) nanoclusters, which can serve as an efficient oxygen reduction through the multi-electron process.[8] In this system, the potential of the valence band (VB) can be kept at deep level with strong oxidation power, and these holes can decompose organic compounds. In other words, this system can take advantage of both the efficient oxygen reduction via Cu(II) nanoclusters and the high oxidation power of the holes in the VB of TiO_2 induced by IFCT under visible light irradiation.[7a−c] These results suggest that some of photocatalytically inactive materials, such as low conduction band materials,[7a] only UV light active materials,[7b] or even some inactive materials, can become good candidates for efficient visible light active photocatalysts by this new concept.

Herein, we demonstrate that the Ti^{3+} self-doped TiO_2 (TiO_2@Ti^{3+}) becomes an efficient visible light active photocatalyst by the grafting of Cu(II) oxide amorphous nanoclusters. This simple and economical method can be extended to apply other defects, such as oxygen vacancies, interstitial Ti, and interstitial O, to develop of a highly active photocatalyst under visible light irradiation.

EXPERIMENTAL SECTION

Synthesis of TiO_2@Ti^{3+} Sample. Different from reduction methods such as the annealing of TiO_2 in vacuum or hydrogen,[5d,9] we developed a facile method for synthesis of stable TiO_2@Ti^{3+} by oxidizing TiO_2 and Ti_2O_3 mixtures in air. Briefly, 1 g powder of Ti_2O_3 (grain size of around 1 μm, specific surface area of 5.4 m^2g^{-1}, Alfa Aesar, 99.8%) and 1 g of commercial TiO_2 powder (rutile form, grain size of 15 nm, specific surface area of 90 m^2g^{-1}, MT-150A, TAYCA Corp.) was mixed and ground into a fine powder using an agate mortar. Then, the mixed powder was heated at 900 °C for 3 h to

Received: October 6, 2011
Published: November 8, 2011

 © 2011 American Chemical Society dx.doi.org/10.1021/cm203025b|*Chem. Mater.* 2011, 23, 5282–5286

form TiO_2@Ti^{3+}. After calcination, the specific surface area of TiO_2@Ti^{3+} is 3.8 m^2/g, which is equal to that of annealed pure TiO_2.[7e] As a control sample, pure TiO_2 was obtained by the same annealing (900 °C for 3 h) onto the commercial TiO_2 powder (MT-150A, TAYCA Corp.).

Grafting of Cu(II) Oxide Amorphous Nanoclusters onto TiO_2@Ti^{3+}. The grafting of Cu(II) oxide amorphous nanoclusters onto TiO_2@Ti^{3+} was performed by the same impregnation method reported previously in ref 7. Briefly, 1 g of TiO_2@Ti^{3+} powder was first dispersed in 10 g of distilled water. $CuCl_2{\cdot}2H_2O$ (Aldrich), acting as the source of Cu(II)-TiO_2@Ti^{3+}, was weighed to give a weight fraction of Cu relative to TiO_2@Ti^{3+} powder of 1×10^{-3}. The weighed $CuCl_2{\cdot}2H_2O$ was then added to the aqueous TiO_2@Ti^{3+} suspension, heated at 90 °C, and stirred for 1 h in a vial reactor. The suspension was then filtered twice with a membrane filter (0.025 μm, Millipore) and washed with sufficient amounts of distilled water. The resulting residues were dried at 110 °C for 24 h and subsequently ground into a fine powder using an agate mortar. The same process was applied for pure TiO_2 to obtain Cu(II)-TiO_2.

Sample Characterization. The crystal structures of the prepared powders were identified by X-ray diffraction (XRD) (Rigaku D/MAX25000, λ=1.54178 Å). The electron spin resonance (ESR) spectra were recorded on a Bruker ESP350E spectrometer. UV–visible absorption spectra were obtained by the diffuse reflection method using a spectrometer (UV-2550, Shimadzu). The morphologies of the samples were investigated by scanning electron microscopy (SEM), using a Hitachi S-4800 apparatus and transition electron microscopy (TEM) on a Hitachi HF-2000 instrument under an acceleration voltage of 200 kV. The specific surface areas of the samples were determined from the nitrogen absorption data at liquid nitrogen temperature, using the Barrett–Emmett–Teller (BET) technique. The samples were degassed at 200 °C and a pressure below 100 mTorr for a minimum of 2 h prior to analysis using a Micromeritics VacPrep 061 instrument. The surface analysis was studied by X-ray photoelectron spectroscopy (XPS; Perkin-Elmer model 5600). The binding energy data are calibrated with the C 1s signal at 284.5 eV.

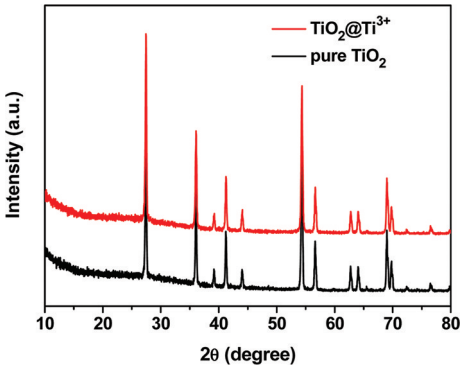

Figure 1. XRD patterns of TiO_2@Ti^{3+} sample and pure TiO_2.

Evaluation of Photocatalytic Activities. The photocatalytic activities of photocatalysts were evaluated by the decomposition of gaseous 2-propanol (IPA) under visible light illumination (400–530 nm, 1 mW/cm^2) from a Xe lamp (LA-251Xe, Hayashi Tokei) equipped with glass filters (L-42, B-47, C-40C, Asahi Techno-Glass). For the analysis, 300 mg of the photocatalyst was uniformly spread over a 5.5-cm^2 irradiation area in a 500-mL quartz vessel. Before injecting 6 μmol (ca. 300 ppm) of gaseous IPA, the organic compounds (originating from the air) absorbed on the surface of catalysts were first photo-oxidized into CO_2 and the gas in the quartz vessel was then replaced with pure synthetic air (N_2/O_2= 80%/20% with the purity of 99.9%). After injecting IPA, the reaction vessel was kept in the dark for 12 h and was then subjected to visible light irradiation to initiate the photocatalytic reactions. The concentrations of acetone and CO_2 produced were monitored using a gas chromatograph (model GC-8A, Shimadzu Co., Ltd.).

RESULTS AND DISCUSSION

Synthesis and Structural Characterization. The obtained TiO_2@Ti^{3+} sample shows a grayish yellow color, while pure TiO_2 exhibits an ordinary white color, as shown in Figure S1 in the Supporting Information. The powder XRD analysis, as shown in Figure 1, shows that the TiO_2@Ti^{3+} sample is a pure rutile phase TiO_2 with high crystallinity. No Ti_2O_3 peaks were detected, which means Ti_2O_3 was oxidized to TiO_2.

ESR and XPS Analysis. To test for the existence of Ti^{3+}, low temperature ESR spectra were recorded, as shown in Figure 2a. The obtained TiO_2@Ti^{3+} showed a clear ESR signal, while no signal was seen for the pure TiO_2. The observed g-values, 1.965, 1.938, and 1.916, are assigned to be paramagnetic Ti^{3+} centers.[4a,b] The ESR data indicate that there is no Ti^{3+} present on the surface of TiO_2@Ti^{3+}. It was demonstrated that surface Ti^{3+} would adsorb atmospheric oxygen to form O^{2-}, and it shows an ESR signal at $g \approx 2.02$.[10] XPS analysis (Figure 2b) also shows no Ti^{3+} signals on the surface of TiO_2@Ti^{3+}. In contrast, pure TiO_2 did not show any ESR signal for Ti^{3+} states. Based on these results, it can be concluded that the origin of Ti^{3+} mainly comes from the oxidized Ti_2O_3.

UV–Vis Spectra. Figure 3a shows the UV–visible absorption spectra for bare and Cu(II) nanoclusters modified TiO_2@Ti^{3+} and pure TiO_2, respectively. The TiO_2@Ti^{3+} exhibited broad visible light absorption, whereas pure TiO_2 did not. According to Kubelka–Munk functions (Figure 3b), the introduction of Ti^{3+} nearly did not narrow the band gap. The Ti^{3+} would be formed as isolated states between the

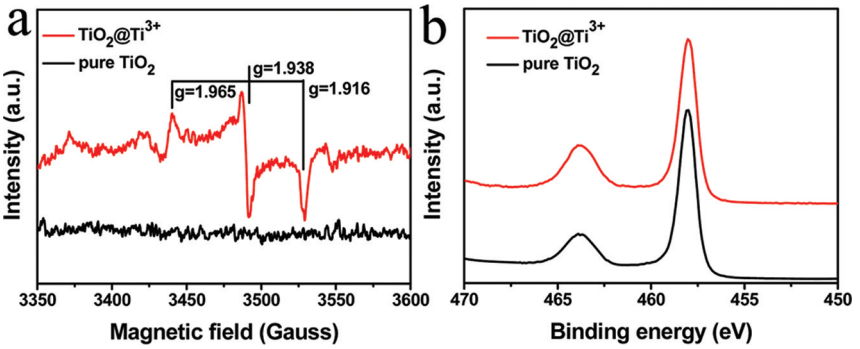

Figure 2. (a) ESR spectra and (b) Ti 2p core-level spectra of TiO_2@Ti^{3+} sample and pure TiO_2.

dx.doi.org/10.1021/cm203025b | Chem. Mater. 2011, 23, 5282–5286

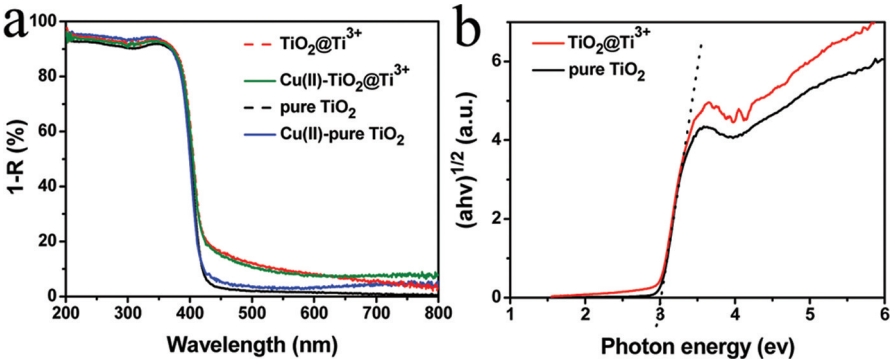

Figure 3. (a) UV−visible absorption spectra of bare and Cu(II) nanoclusters grafted TiO_2@Ti^{3+} and pure TiO_2, respectively. The dash curves correspond to those of the bare samples. (b) Plots of the square root of the Kubelka−Munk function against photon energy.

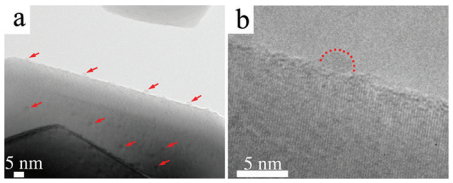

Figure 4. (a) TEM and (b) HRTEM images of Cu(II)-TiO_2@Ti^{3+}. Nanoclusters (marked by red arrows) were highly dispersed on the TiO_2@Ti^{3+} surface. In part b, a short dashed curve is applied to outline the Cu(II) nanoclusters. The good attachment of nanoclusters and TiO_2@Ti^{3+} can be clearly observed.

forbidden gap. This isolated band has various electric levels from 0.3 to 0.8 eV below the conduction band minimum.[5c,d] Therefore, TiO_2@Ti^{3+} exhibited broad visible light absorption.[3]

As shown in Figure 3a, it is clearly shown that, for Cu(II)-TiO_2, the grafting of Cu(II) nanoclusters increases the absorption intensities in the 420−550 and 700−800 nm wavelength regions. The slight increase in the former region can be assigned to IFCT of VB electrons to surface-grafted Cu(II) nanoclusters, as we reported previously in the Cu(II)-TiO_2 system, and the latter is due to a simple d-d transition of Cu(II).[7a−d] In contrast, for Cu(II)-TiO_2@Ti^{3+}, the grafting of Cu(II) nanoclusters slightly decreases the absorption intensities in the 420−550 nm wavelength region, while the increases of the absorption intensities can also be observed in the 700−800 nm wavelength region because of d-d transition of Cu(II). These results indicate that the IFCT absorption is masked, owing to the strong visible light absorption of TiO_2@Ti^{3+}.

TEM Analysis. Figure 4a shows a TEM image of Cu(II)-TiO_2@Ti^{3+}. It clearly shows that the Cu(II) nanoclusters, in the size of ∼2 nm, are well dispersed on the surfaces of TiO_2@Ti^{3+}. The good attachment of Cu(II) nanoclusters to the high crystallized TiO_2@Ti^{3+} surfaces with the clear lattice fringes of the rutile phase are observed from the high resolution TEM (HRTEM) images (Figure 4b). Point analysis of energy dispersive X-ray spectroscopy (EDS, Figure S2 in the Supporting Information) and surface analysis of XPS (Figure S3 in the Supporting Information) proved that these nanoclusters are composed of Cu.

Photocatalytic Activity. Even though an isolated band of Ti^{3+} states contribute to the visible light absorption, isolated states usually act as recombination centers.[4,5,11]

As shown in Figure 5a, without nanocluster grafting, TiO_2@Ti^{3+} has a negligible activity either under visible light or UV light irradiation, with the same absorbed photon numbers condition as that of Cu(II)-TiO_2@Ti^{3+} under the visible light irradiation. In contrast, grafting Cu(II) nanoclusters switched these powders to an efficient photocatalyst. Figure 5b shows the photocatalytic activities of Cu(II)-TiO_2@Ti^{3+} and Cu(II)-TiO_2, evaluated by monitoring the acetone and CO_2 concentrations generated by the gaseous decomposition of IPA under visible light (400−530 nm, 1 mW/cm^2). Photocatalytic decomposition of gaseous IPA requires strong oxidation power of holes for the complete decomposition, rather than some dye molecules, and proceeds via formation of acetone as an intermediate, followed by further decomposition of acetone to the final products CO_2 and H_2O.[12] With the onset of visible light irradiation, the Cu(II)-TiO_2@Ti^{3+} produced both acetone and CO_2 efficiently, as compared to the Cu(II)-TiO_2. The CO_2 generation rate of the Cu(II)-TiO_2@Ti^{3+} is 0.20 μmol/h, which is much larger than that of the bare TiO_2@Ti^{3+} (0.004 μmol/h) and that of the Cu(II)-TiO_2 (0.09 μmol/h). The Cu(II)-TiO_2@Ti^{3+} could completely decompose the gaseous IPA to finally produce the CO_2 with the amount of ∼18 μmol.[7] This photocatalyst was very stable; that is, its efficient visible light activity was maintained even after it was repeatedly used in air for 6 months (Figure S4 in the Supporting Information). The quantum efficiency (QE) for CO_2 generation on Cu(II)-TiO_2@Ti^{3+} was calculated to be ca. 10.8% (the calculation details are described in ref 7 and in Figure S5 in the Supporting Information), which was comparable to the performance of WO_3 based photocatalyst.[7a,d] Furthermore, in the present study, visible light absorption is increased by introducing the Ti^{3+} sites into the TiO_2 in addition to the IFCT absorption. The light absorption capability of our Cu(II)-TiO_2@Ti^{3+} in the 400−530 nm region increased to 1.85×10^{15} quanta·s^{-1}, which is equal to that of our Cu(II) nanoclusters grafted conduction band (CB) controlled TiO_2 ($Ti_{1-3x}W_xGa_{2x}O_2$),[7c] ca. 1.9 times, relative to Cu(II)-TiO_2.

We also investigated the photocatalytic activity of our Cu(II)-TiO_2@Ti^{3+} under UV irradiation with the same absorbed photon numbers conditions as that under the visible light irradiation. It can be found that its activity under visible light is similar to that under UV light (Figure S6 in the Supporting Information). Further, it is noteworthy that the UV light activity of our Cu(II)-TiO_2@Ti^{3+} is comparable to that of one of the commercially available efficient photocatalytic TiO_2, (ST-01, Ishihara Sangyo Co. Ltd., Figure S6 in the Supporting

dx.doi.org/10.1021/cm203025b|*Chem. Mater.* 2011, 23, 5282−5286

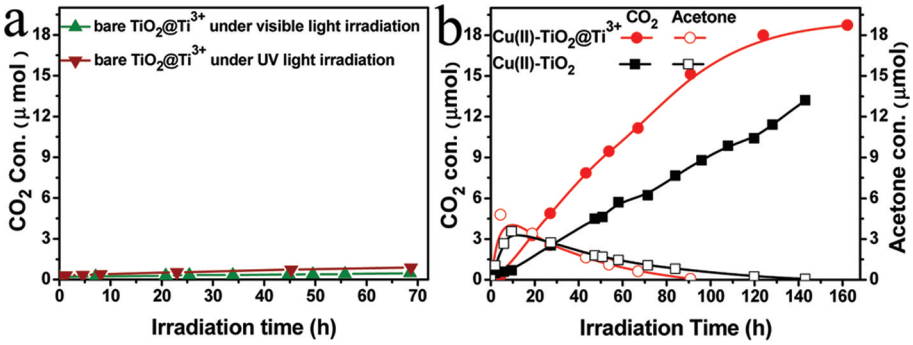

Figure 5. (a) Photocatalytic activities of the TiO_2@Ti^{3+} sample without Cu(II) nanoclusters co-catalyst under visible light and UV irradiation. (b) Time-dependent gas concentrations during IPA decomposition over Cu(II)-TiO_2@Ti^{3+} and Cu(II)-TiO_2 photocatalysts under visible light irradiation at 400−530 nm (1 mW/cm^2).

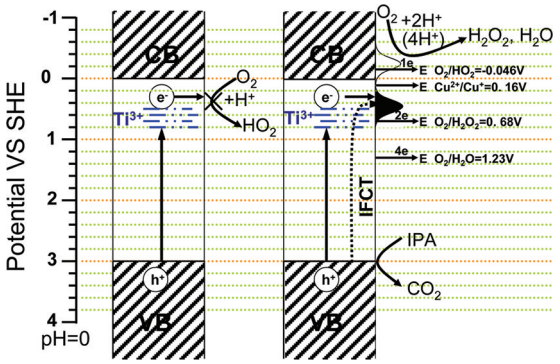

Figure 6. Proposed photocatalysis processes.

Information). These results also reveal that the Cu(II) nanoclusters co-catalysts suppress the recombination under visible and UV light irradiation.

Photocatalytic Mechanisms. It has been reported that the Ti^{3+} can produce isolated states in the forbidden gap.[6] Therefore, TiO_2@Ti^{3+} exhibits visible light absorption.[4] These Ti^{3+} defects are occupied states and usually act as donors.[13] The electrons in these sites are excited to CB by a thermal or photoexcitation process to form the unoccupied states.[14] This process corresponds to the light absorption at the wavelength over 600 nm, as shown in Figure 2a. At the same time, the electrons in the VB can be excited to these unoccupied sites. However, these Ti^{3+} sites are electron traps; thus, photogenerated charge carriers are easily recombined at these sites.[4−6] As a result, Ti^{3+} deteriorates its photocatalytic activity under UV light as well as under visible light. Once the sample was grafted with Cu(II) nanoclusters, the potential of the Cu^{2+}/Cu^{+} is about 0.16 V (vs SHE, pH = 0), which can be expected to act as a co-catalyst.[7a−d] Visible light irradiation induced electrons on an isolated Ti^{3+} band can be transferred to the surface Cu(II) nanoclusters efficiently, in addition to the direct charge transfer from the VB to the Cu(II) nanoclusters. Therefore, for Cu(II)-TiO_2@Ti^{3+}, under visible light irradiation, the holes in the VB decomposed IPA, while photoinduced electrons were transferred to the surface Cu(II) nanoclusters and consumed via oxygen reduction process efficiently,[8] which accounts for the enhanced activity compared to bare TiO_2@Ti^{3+}. As a result, TiO_2@Ti^{3+}, which was once considered to be photocatalytically inactive, became an efficient visible-light-sensitive photocatalyst. On the basis of these results, the photocatalytic mechanisms are speculated in Figure 6.

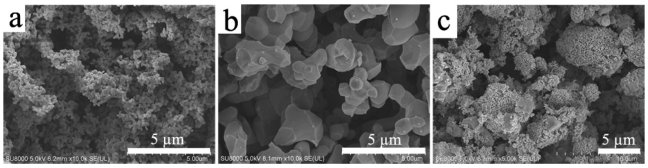

Figure 7. SEM images of (a) pure annealed TiO_2, (b) pure oxidized Ti_2O_3, and (c) TiO_2@Ti^{3+} sample, respectively.

Experimental Parameters Influences. It is noted that the starting material (Ti_2O_3 and TiO_2 mixture) is very important for synthesizing TiO_2@Ti^{3+}. If we used single component of Ti_2O_3 powder as a starting material, it showed much more enhanced visible light absorption (Figure S7 in the Supporting Information). However, its photocatalytic activity was very low (Figure S8 in the Supporting Information). These results indicate that the morphology and the degree of oxidation states are important to achieve an efficient visible light activity. When the starting material is pure Ti_2O_3, Ti^{3+} ions are mainly located at the deeper position of the large oxidized Ti_2O_3 particles after the annealing in air, and the oxidized pure Ti_2O_3 shows very low photocatalytic activity.[4a] However, for our TiO_2@Ti^{3+}, small TiO_2 nanoparticles uniformly covered large oxidized Ti_2O_3 particles (Figure 7), and the oxygen can diffuse between these particles under heat treatment in air with high temperature.

We have optimized the various experimental conditions like the ratio between the amount of TiO_2 and Ti_2O_3 and annealing temperature, as shown in Figure 8. The results in Figure 5 demonstrate our best performance for visible light activity. It may be due to the annealing temperature, and the ratio of TiO_2 to Ti_2O_3 seriously influences the morphology and the degree of oxidation states, which are important for efficient visible light activity.

■ CONCLUSION

In summary, we developed a simple method to convert photochemically inactive TiO_2@Ti^{3+} into an efficient visible-light-sensitive photocatalyst by the grafting of Cu(II) oxide amorphous nanoclusters. The visible light absorption was enhanced by introducing Ti^{3+} ions in the TiO_2. After the grafting of Cu(II) oxide amorphous nanoclusters, these nanoclusters suppressed the recombination of electron−hole pairs at the isolated Ti^{3+} band, and these Cu(II) oxide amorphous nanoclusters acted as a co-catalyst for efficient

dx.doi.org/10.1021/cm203025b|Chem. Mater. 2011, 23, 5282−5286

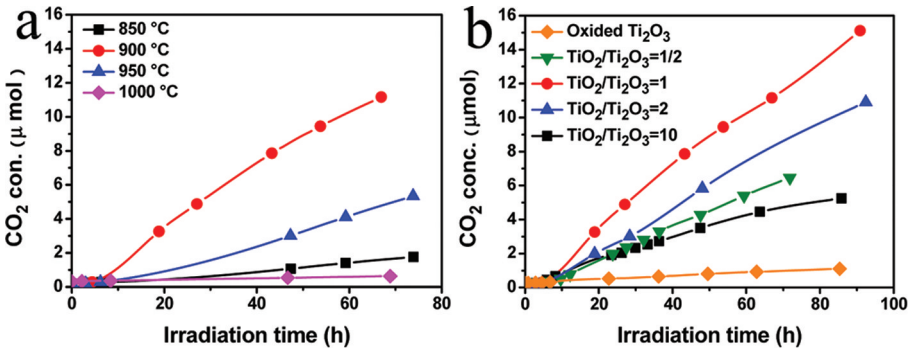

Figure 8. Photocatalytic activities of Cu(II)-TiO_2@Ti^{3+} under visible light irradiation at 400−530 nm (1 mW/cm^2) with different (a) annealing temperatures and (b) ratios between the amount of TiO_2 and Ti_2O_3.

oxygen reduction to consume the photoinduced electrons. Therefore, the photocatalytic activity of the Cu(II)-TiO_2@Ti^{3+} increased drastically under either UV or visible light irradiation, and it can completely decompose gaseous IPA, even under visible light irradiation. This photocatalyst is very stable in air and can be repeatedly used without degradation in the visible light activity. Furthermore, this simple and economical method can be extended to apply other defects, such as oxygen vacancies, interstitial Ti, and interstitial O, to develop of a highly active photocatalyst under visible light irradiation.

■ ASSOCIATED CONTENT

Ⓢ Supporting Information

Photos, EDS analysis, XPS analysis, UV−vis spectra, stability, UV light irradiation photocatalytic activity of samples, and the quantum efficiency calculation details. This material is available free of charge via the Internet at http://pubs.acs.org.

■ AUTHOR INFORMATION

Corresponding Author

*E-mail: mmiyauchi@ceram.titech.ac.jp (M. M.); hashimoto@light.t.u-tokyo.ac.jp (H. K.).

■ ACKNOWLEDGMENTS

This work was performed under the management of the Project to Create Photocatalysts Industry for Recycling-Oriented Society supported by the New Energy and Industrial Technology Development Organization (NEDO) in Japan.

■ REFERENCES

(1) Fujishima, A.; Honda, K. *Nature* **1972**, *238*, 37.
(2) (a) Linsebigler, A. L.; Lu, G. Q.; Yates, J. T. Jr. *Chem. Rev.* **1995**, *95*, 735. (b) Chen, X. B.; Mao, S. S. *Chem. Rev.* **2007**, *107*, 2891.
(3) (a) Liu, H. M.; Yang, W. S.; Ma, Y.; Yao, J. N. *Appl. Catal., A* **2006**, *299*, 218. (b) Zuo, F.; Wang, L.; Wu, T.; Zhang, Z.; Borchardt, D.; Feng, P. *J. Am. Chem. Soc.* **2010**, *132*, 11856. (c) Martyanova, I. N.; Bergerb, T.; Diwaldb, O.; Rodriguesa, S.; Klabunde, K. J. *J. Photochem. Photobiol., A* **2010**, *212*, 135.
(4) (a) Nakaoka, Y.; Nosaka, Y. *J. Photochem. Photobiol., A* **1997**, *110*, 299. (b) Bonneviot, L.; Haller, G. L. *J. Catal.* **1988**, *113*, 96. (c) Lo, W. J.; Chung, Y. W.; Somorjai, G. A. *Surf. Sci.* **1978**, *71*, 199. (d) Chen, W.; Cameron, S.; Gdthelid, M.; Hammar, M.; Paul., J. *J. Phys. Chem.* **1995**, *99*, 12892. (e) Liu, G.; Rodriguez, J. A.; Hrbek, J.; Long, B. T.; Chen, D. A. *J. Mol. Catal. A: Chem:* **2003**, *202*, 215. (f) Ohtani, B.; Ogawa, Y.; Nishimoto, S. I. *J. Phys. Chem. B: Enzym.* **1997**, *101*, 3746.
(5) (a) Ghosh, A. K.; Wakim, F. G.; Addiss, P. R. *Phys. Rev. Lett.* **1969**, *184*, 979. (b) Shultz, A. N.; Jang, W.; Hetherington, W. M. III; Baer, D. R.; Wang, L.; Engelhard, M. H. *Surf. Sci.* **1995**, *339*, 114. (c) Valentin, D. C.; Pacchioni, G.; Selloni, A. *J. Phys. Chem. C* **2009**, *113*, 20543. (d) Thompson, T. L.; Yates, J. T. Jr. *Chem. Rev.* **2006**, *106*, 4428.
(6) Cronemeyer, D. C. *Phys. Rev.* **1959**, *113*, 1222.
(7) (a) Irie, H.; Miura, S.; Kamiya, K.; Hashimoto, K. *Chem. Phys. Lett.* **2008**, *457*, 202. (b) Irie, H.; Kamiya, K.; Shibanuma, T.; Miura, S.; Tryk, D. A.; Yokoyama, T.; Hashimoto, K. *J. Phys. Chem. C* **2009**, *113*, 10761. (c) Yu, H. G.; Irie, H.; Hashimoto, K. *J. Am. Chem. Soc.* **2010**, *132*, 6899. (d) Qiu, X. Q.; Miyauchi, M.; Yu, H.; Irie, H.; K. Hashimoto, K. *J. Am. Chem. Soc.* **2010**, *132*, 15259. (e) Yu, H. G.; Irie, H.; Shimodaira, Y.; Hosogi, Y.; Kuroda, Y.; Miyauchi, M.; Hashimoto, K. *J. Phys. Chem. C* **2010**, *114*, 16481.
(8) (a) Himo, F.; Eriksson, L. A.; Maseras, F.; Siegbahn, P. E. M. *J. Am. Chem. Soc.* **2000**, *122*, 8031. (b) Goldstein, S.; Czapski, G.; Eldik, R.; Cohen, H.; Meyerstein, D. *J. Phys. Chem.* **1991**, *95*, 1282. (c) Kitajima, N.; Morooka, Y. *Chem. Rev.* **1994**, *94*, 737. (d) Cole, A. P.; Root, D. E.; Mukherjee, P.; Solomon, E. I.; Stack, T. D. P. *Science* **1996**, *273*, 1848.
(9) Ganduglia-Pirovano, M. V.; Hofmann, A.; Sauer, J. *Surf. Sci. Rep.* **2007**, *62*, 219.
(10) (a) Howe, R. F.; Gratzel, M. *J. Phys. Chem.* **1987**, *91*, 3906. (b) Anpo, M.; Che, M.; Fubini, B.; Garrone, E.; Giamello, E.; Paganini, M. C. *Top. Catal.* **1999**, *8*, 189. (c) Komaguchi, K.; Maruoka, T.; Nakano, H.; Imae, I.; Ooyama, Y.; Harima, Y. *J. Phys. Chem. C* **2009**, *113*, 1160.
(11) (a) Herrmann, J. M.; Disdier, J.; Pichat, P. *Chem. Phys. Lett.* **1984**, *108*, 618. (b) Luo, Z.; Gao, Q. H. *J. Photochem. Photobiol., A* **1992**, *63*, 367. (c) Herrmann, J. M. *Top. Catal.* **2006**, *39*, 3. (d) Herrmann, J. M. *Appl. Catal., B* **2010**, *99*, 461. (e) Jung, K. Y.; Park, S. B.; Ihm, S. K. *Appl. Catal., B* **2004**, *51*, 239. (f) Dozzi, M. V.; Livraghi, S.; Giamello, E.; Selli, E. *Photochem. Photobiol. Sci.* **2011**, *10*, 343.
(12) (a) Ohko, Y.; Hashimoto, K.; Fujishima, A. *J. Phys. Chem. A* **1997**, *101*, 8057. (b) Ohko, Y.; Fujishima, A.; Hashimoto, K. *J. Phys. Chem. B* **1998**, *102*, 1724. (c) Ohko, Y.; Try, D. A.; Hashimoto, K.; Fujishima, A. *J. Phys. Chem. B* **1998**, *102*, 2699.
(13) (a) Weidmann, J.; Dittrich, T.; Konstantinova, E.; Lauermann, I.; Uhlendorf, I.; Koch, F. *Sol. Energy Mater. Sol. Cells* **1999**, *56*, 153. (b) Toyoda, T.; Hayashi, M. *Rev. Sci. Instrum.* **2003**, *74*, 337. (c) Eder, D.; Kramer, R. *Phys. Chem. Chem. Phys.* **2003**, *5*, 1314. (d) Lisachenko, A. A.; Mikhailov, R. V.; Basov, L. L.; Shelimov, B. N.; Che, M. *J. Phys. Chem. C* **2007**, *111*, 14440.
(14) Dimitar, A. P.; Yates, J. T. Jr. *Chem. Phys. Lett.* **2007**, *436*, 204.